7-31-2018

Hybrid Cell Outage Compensation in 5G Networks: Sky-Ground Approach

Mohamed Y. Selim
Iowa State University, myoussef@iastate.edu

Ahmad Alsharoa
Iowa State University

Ahmed E. Kamal
Iowa State University, kamal@iastate.edu

Hybrid Cell Outage Compensation in 5G Networks: Sky-Ground Approach

Abstract

Unmanned Aerial Vehicles (UAVs) enabled communications is a novel and attractive area of research in cellular communications. It provides several degrees of freedom in time, space and it can be used for multiple purposes. This is why wide deployment of UAVs has the potential to be integrated in the upcoming 5G standard. In this paper, we present a novel cell outage compensation (COC) framework to mitigate the effect of the failure of any outdoor Base Station (BS) in 5G networks. Within our framework, the outage compensation is done with the assistance of sky BSs (UAVs) and Ground BSs (GBSs). An optimization problem is formulated to jointly minimize the energy of the Drone BSs (DBSs) and GBSs involved in the healing process which accordingly will minimize the number of DBSs and determine their optimal 2D positions. In addition, the DBSs will mainly heal the users that the GBS cannot heal due to capacity issues. Simulation results show that the proposed hybrid approach outperforms the conventional COC approach. Moreover, all users receive the minimum quality of service in addition to minimizing the UAVs' consumed energy.

Keywords

Self-healing, Cell Outage Compensation, Drone-based Communications, Unmanned Aerial Vehicles (UAVs), 5G

Disciplines

Systems and Communications

Comments

This is a manuscript of a proceeding published as Selim, Mohamed Y., Ahmad Alsharoa, and Ahmed E. Kamal. "Hybrid Cell Outage Compensation in 5G Networks: Sky-Ground Approach." In *2018 IEEE International Conference on Communications (ICC)*, (2018): 1-6. DOI: 10.1109/ICC.2018.8422155. Posted with permission.

Hybrid Cell Outage Compensation in 5G Networks: Sky-Ground Approach

Mohamed Y. Selim, Ahmad Alsharoa and Ahmed E. Kamal
Iowa State University, Iowa State, USA, Email: {myoussef, alsharoa, kamal}@iastate.edu

***Abstract*—Unmanned Aerial Vehicles (UAVs) enabled communications is a novel and attractive area of research in cellular communications. It provides several degrees of freedom in time, space and it can be used for multiple purposes (self-healing, offloading, relaying or coverage extension). This is why wide deployment of UAVs has the potential to be integrated in the upcoming 5G standard. In this paper, we present a novel cell outage compensation (COC) framework to mitigate the effect of the failure of any outdoor Base Station (BS) in 5G networks. Within our framework, the outage compensation is done with the assist of sky BSs (UAVs) and Ground BSs (GBSs). An optimization problem is formulated to jointly minimize the energy of the Drone BSs (DBSs) and GBSs involved in the healing process which accordingly will minimize the number of DBSs and determine the optimal 2D positions of them. In addition, the DBSs will mainly heal the users that the GBS can't heal due to capacity issues. Simulation results proved that the proposed hybrid approach outperforms the conventional COC approach. Moreover, all users received the minimum quality of service in addition to minimizing the UAVs' consumed energy.**

***Index Terms*—Self-healing, Cell Outage Compensation, Drone-based Communications, Unmanned Aerial Behicles (UAVs), 5G.**

I. Introduction

Unmanned aerial vehicles (UAVs) enabled communications have attracted considerable attention recently due to the inherent agility [1]. On demand, UAVs can rapidly provide network access to be used in various applications. As reported by AIAA (www.aiaa.org), the global market for commercial UAV applications will skyrocket to as much as 127 billion dollars by 2020. UAVs, also known as drones, are gaining increasing popularity in Information Technology (IT) applications due to their high flexibility for on-demand deployments. Several leading IT companies have launched pilot projects. According to Nokia (www.nokia.com), in May 2016, they launched a rapidly deployable 4G solution that can be carried by a drone to provide connectivity at high-traffic events. Also, project Loon by Google (www.google.com/loon) provided internet access worldwide by leveraging the UAV/drone technology. There are other pilot projects lead by other companies such as Facebook and AT&T.

In particular, employing UAVs as aerial Base-Stations (BSs) is envisioned as a promising solution to tackle the challenges facing the existing, 4G, and the upcoming, 5G, networks. One of the main challenges facing these networks is the failure of the BSs and how to self-heal or mitigate this failure in an autonomous way. A Self Organizing Network (SON) aims to leapfrog the overall performance of the network to a higher level of automated operation. SON defines three areas: self-configuration, self-optimization and self-healing [2].

Self-healing is the execution of actions that keep the network operational and/or prevent disruptive problems from arising. Self-healing is done in two steps: Cell Outage Detection (COD) and Cell Outage Compensation (COC). The COD is to detect and classify failures, while minimizing the detection time. The COC executes actions to mitigate or, at least, alleviate the effect of the failure [3].

When a failure occurs to any BS in the network, the conventional and well-known cell outage compensation technique is to change the neighboring BSs antenna tilt and power to serve the users of the failed BS. The advantage of this self-healing technique is that it is very fast and guarantees minimum Quality of Service (QoS) to the users under the failed BS. However, the disadvantage of this technique is that the users of the neighboring BSs will be affected by the change in their BS's antenna configuration.

To make use of the advantage of the conventional self-healing technique and avoid its disadvantage, we propose a novel approach where the DBSs will serve users that are not connected to any neighboring GBS or those users that overloading neighboring GBS and affecting its original users. Since DBS is consuming more energy in the healing process than the GBSs, due to hardware and hovering energy, we only use DBSs in these two cases only. This is achieved by minimizing the energy of the healing process which consequently will minimize the number of used DBSs and ensure that each user is attached at least to one BS (either DBS or GBS) and receiving the minimum required achievable rate.

Although there has been significant amount of work on using DBSs in cellular networks, using DBSs in self-healing is still at its infancy.

In [4], the positioning of aerial relays is discussed to compensate cell outage and cell overload. The authors in [5] show the improvement in the coverage by assisting the network with DBSs at a certain altitude, in case of failure of the network BS.

In [6], the optimal altitude of a drone-BS that achieves a required coverage with minimum transmission power is found. Also providing maximum coverage with two DBSs in the presence and absence of interference is investigated.

The authors in [7], the authors designed an offloading scheme using UAVs where UAVs flies cyclically along the cell edge to serve cell-edge users and help offload data from the GBS.

The rest of this paper is organized as follows. Section II introduces the system model. In Section III, the optimization problem and its proposed solution is presented. Section IV presents the numerical results to demonstrate the performance of the proposed approach. Finally, the paper is concluded in Section V.

II. System Model

As shown in Fig. 1, we consider a wireless communication system with a heterogeneous network and $D \geq 1$ Drone Base-Stations (DBSs) which are employed to heal a group of U ≥ 1 UEs under the failed BS given one failure at a time or multiple failures in different geographical locations.

The set $\mathcal{U} = \{1, 2, \ldots, U\}$ denotes the set of active UEs under the failed BS and they are at known locations where the horizontal coordinate of each UE u is fixed at $\mathbf{g}_u = [x_u, y_u]^T \in \mathbb{R}^{2\text{x}1}$, $u \in U$, assuming that all UEs are having zero altitude. The set $\mathcal{D} = \{1, 2, \ldots, D\}$ denotes the set of DBSs used to heal the failed BS where all DBSs are assumed to navigate at a fixed altitude h and the horizontal coordinate of DBS $d \in D$ at discrete time instant n where $n = 1, ..., N$ is denoted by $\mathbf{J}_d^n = [x_d^n, y_d^n]^T \in \mathbb{R}^{2\text{x}1}$ where N is a total discrete period.

We denote that DBS d is used in time block n by κ_d^n which acts as a decision variable in our optimization problem formulation. The UEs under the failed BS are associated to either a DBS or a Ground Base-Station (GBS). We denote $\zeta_{u,d,m}^n$ as the binary variable which indicate that UE u is associated to DBS d and using sub-channel m during time block n. Similarly, $\epsilon_{u,l,m}^n$ is defined for GBS l. In other words, $\epsilon_{u,l,m}^n = 1$ if UE u is associated to GBS l using sub-channel m during time block n, and $\epsilon_{u,l,m}^n = 0$ otherwise.

Assume that the DBS-UE communication channels are dominated by LoS links. Though simplified, the LoS model offers a good approximation for practical Drone-UE channels and enables us to investigate the main objective of the optimization problem presented later. Under the LoS model, the Drone-UE channel power gain follows the free space path loss model which is determined mainly by the DBS-UE distance. Given that $\mathbf{J}_d^n$, $\mathbf{J}_l$ and g_u as the coordinates of DBS d, GBS j and UE u in the horizontal plane at discrete time instant n, respectively, then the distance from DBS d to UE u in time block n can be expressed as:

$$\delta_{u,d}^n = \sqrt{h_d^2 + ||\mathbf{J}_d^n - \mathbf{g}_u||^2} \tag{1}$$

Similarly, the distance from GBS l to UE u in time block n can be expressed as:

$$\delta_{u,l} = \sqrt{h_l^2 + ||\mathbf{J}_l - \mathbf{g}_u||^2} \tag{2}$$

where $\mathbf{J}_l$ is constant similar to $\mathbf{g}_u$, h_l is the height of the GBS and we assume that the height of the UEs is considered to be zero.

A. DBS and GBS Channel and Achievable Rate Models

For simplicity, we assume that the communication links DBS-UE are dominated by the LoS links where the channel quality depends only on the distance between the DBS and the UE. Under this LoS model, the DBS-UE channel power gain mainly follows the free space path loss model which is given as follows:

$$\Gamma_{u,d}^n = \rho_o(\delta_0/\delta_{u,d}^n)^2 = \frac{\rho_o}{h^2 + ||\mathbf{J}_d^n - \mathbf{g}_u||^2} \tag{3}$$

where ρ_o is a unitless constant that depends on the antenna characteristics and frequency and measured at the reference distance $\delta_0 = 1$ m. Moreover, we assume that the channel gain for the communication links GBS-UE are following the urban path loss model which is given by:

$$\Gamma_{u,l} = \rho_o(\delta_0/\delta_{u,l})^\alpha = \frac{\rho_o}{\left(\sqrt{h_l^2 + ||\mathbf{J}_l - \mathbf{g}_u||^2}\right)^\alpha} \tag{4}$$

Let $\mathcal{M} = \{1, 2, \ldots, M\}$ be the set of self-healing sub-channels that each DBS and GBS can use during the self-healing process. These sub-channels will be further divided and allocated to the UEs associated to each DBS and GBS. We assume that each DBS d and GBS l transmit with a constant per sub-channel transmit power $p_{d,m}$ and $p_{l,m}$, respectively. If sub-channel m is not assigned to DBS d then $p_{d,m}$ will be zero. For simplicity, we assume that there is no interference between the DBS tier and the GBS tier which means that each of them is using different sets of sub-channels. Hence, the received Signal to Interference plus Noise Ratio (SINR) between DBS d and UE u per sub-channel m during time block n can be expressed as:

$$\gamma_{u,d,m}^n = \frac{p_{d,m}\ \Gamma_{u,d}^n}{\sum\limits_{\substack{j \in \mathcal{D} \\ j \neq d}} p_{j,m} \Gamma_{u,j}^n + \sigma^2} = \frac{\frac{p_{d,m}\ \rho_o}{h^2 + ||\mathbf{J}_d^n - \mathbf{g}_u||^2}}{\sum\limits_{\substack{j \in \mathcal{D} \\ j \neq d}} \frac{p_{j,m}\ \rho_o}{h^2 + ||\mathbf{J}_j^n - \mathbf{g}_u||^2} + \sigma^2} \tag{5}$$

Similarly, we can express the received SINR between GBS l and UE u per sub-channel m during time block n as:

$$\gamma_{u,l,m} = \frac{p_{l,m}\ \Gamma_{u,l}}{\sum\limits_{\substack{i \in \mathcal{L} \\ i \neq l}} p_{i,m} \Gamma_{u,i} + \sigma^2} = \frac{\frac{p_{l,m}\ \rho_o}{\left(\sqrt{h_l^2 + ||\mathbf{J}_l - \mathbf{g}_u||^2}\right)^\alpha}}{\sum\limits_{\substack{i \in \mathcal{L} \\ i \neq l}} \frac{p_{i,m}\ \rho_o}{\left(\sqrt{h_l^2 + ||\mathbf{J}_l - \mathbf{g}_u||^2}\right)^\alpha} + \sigma^2} \tag{6}$$

where σ^2 is the power of the Additive White Gaussian Noise (AWGN) at the receiver. The first term in the denominator of equations (5) and (6) represents the co-channel interference caused by the transmissions of all other DBS/GBSs on the same sub-channel m, respectively. Thus the achievable per sub-channel rate of UE u connected to DBS d during time block n is $R_{u,d,m}^n = \log_2(1 + \gamma_{u,d,m}^n)$ bps/Hz. Moreover, the achievable per sub-channel rate of UE u connected to GBS l during time block n is $R_{u,l,m} = \log_2(1 + \gamma_{u,l,m})$ bps/Hz.

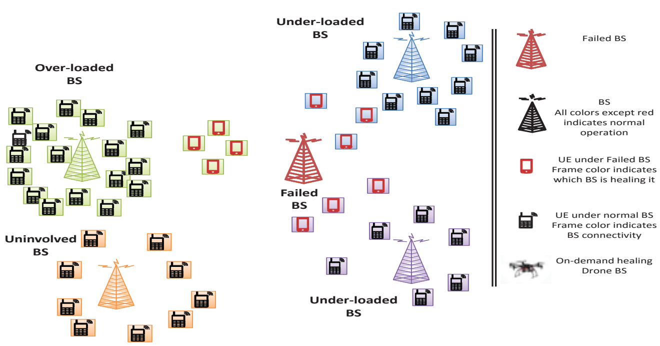

Figure 1 : Conventional self-healing approach.

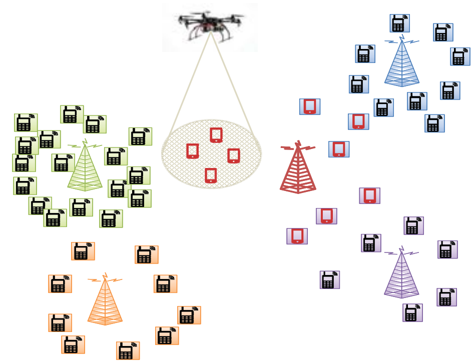

Figure 2 : Hybrid self-healing approach.

B. Base Stations Power Model

In order for any GBS to serve its connected users during a time block n, GBS l consumes a certain amount of power. This amount of power can be expressed as [10]:

$$P_l^{n(noSH)} = \alpha_l P_{U_N} + \beta_l, \tag{7}$$

where α_l is the scaling parameter, U_N is the total number of users served by the GBS in normal operation, i.e., no self-healing (noSH), P_{U_N} is the total power used by this GBS to serve all its users during normal operation and β_l models a constant power which is consumed independently of the radiated power of GBS.

Upon the failure of any BS, the neighboring GBSs will heal the users under the failed BS by applying the conventional self-healing approach, i.e., changing antenna tilt and power. The additional power consumed by neighboring GBS l during the self-healing period $P_l^{n(SH)}$ is the power radiated to heal those users. This can be expressed as:

$$P_{l,m}^{n(SH)} = \tilde{\alpha}_l \sum_{u=1}^{U} \epsilon_{u,l,m}^n p_{l,m} \tag{8}$$

where $\tilde{\alpha}_l$ is a scaling parameter which takes into consideration the change (increase) of the BS antenna power during the healing process where $\tilde{\alpha}_l \geq \alpha_l$. $\epsilon_{u,l,m}^n$ is a binary variable indicating the association of the user u with BS l using sub-channel m and $p_{l,m}$ is the fixed amount of power radiated from the GBS to each user connected to it. Note that the additional independent power β_l is not accounted in the case of failure since this power is already consumed whether there is a failure or no and in Eq (8) we are only considering the excess consumed power due to the healing process.

C. Drone Power Model

There are three sources draining power from the DBS battery: 1) The hardware power 2) The hovering power 3) The DBS transmission power. We assume that all drones move with a fixed speed denoted by v_d. The hovering and hardware drone power levels, denoted by P_{hov} and P_{har}, can be expressed, respectively, as [11]:

$$P_{\text{hov}} = \sqrt{\frac{(m_{\text{tot}} g)^3}{2\pi r_p^2 n_p \rho}}, \tag{9}$$

$$P_{\text{har}} = \frac{P_{\text{full}} - P_s}{v_{\text{max}}} v_d + P_s, \tag{10}$$

where m_{tot}, g, and ρ are the drone mass in (Kg), earth gravity in (m/s^2), and air density in (Kg/m^3), respectively. r_p and n_p are the radius and the number of the drone's propellers, respectively. v_{max} is the maximum speed of the drone and in our model it is equal to v_d. P_{full} and P_s are the hardware power levels when the drone is moving at full speed and when the drone is in idle mode, respectively. When the DBS is flying to a destination, it will consume P_{har}. Finally, the total flying power of DBS d can be calculated as $P_f = P_{\text{hov}} + P_{\text{har}}$.

The DBS transmission power can be modeled exactly in the same way of the regular BS with the new parameters α_d and β_d. This can be seen in the second term of equation (12).

III. Problem Formulation and Proposed Solution

In this section, we formulate an optimization problem aiming to minimize the total energy of the healing GBSs and DBSs during the hybrid self-healing mechanism which will determine when to use DBSs in the proposed healing scheme given capacity and rate constraints. The optimization problem starts after the detection of the failure and hence applying the conventional self-healing technique (neighboring GBSs will serve the UEs originally served by the failed BS) to serve the affected UEs. Once all UEs are served by the neighboring GBSs, the optimization problem will work mainly on minimizing the overall system energy, hence minimizing the number of DBSs used in the healing process.

The total energy consumed by BS l to heal the UEs of the failed BS during time block n is given by the total duration of healing T multiplied by the healing power as follows:

$$E_{l,m}^n = T P_l^{n(SH)} = T\tilde{\alpha}_l \sum_{u=1}^{U} \epsilon_{u,l,m}^n p_{l,m} \tag{11}$$

The total energy consumed by any DBS d to heal the users of the failed BS is given by:

$$E_{d,m}^n = \kappa_d^n \big(T_f(P_{\text{har}}) + T(P_{\text{har}} + P_{\text{hov}})\big) + T[\alpha_d \sum_{u=1}^{U} \zeta_{u,d,m}^n \, p_{d,m} + \beta_d] \tag{12}$$

where κ_d^n is a binary variable indicating whether or not DBS d is used in time block n and T_f is the time the DBS takes to travel from its initial position to the position from which it will serve the users.

A. Problem Formulation

The optimization problem minimizing the energy of the healing BSs (ground and sky BSs) to heal the UEs under the failed OSC is given by:

$$(\mathbf{P1}): \underset{\mathbf{J_d^n}, \epsilon_{u,l,m}^n, \zeta_{u,d,m}^n, \kappa_d^n}{\text{minimize}} \sum_{n=1}^{N} \sum_{l=1}^{L} \sum_{m=1}^{M} E_{l,m}^n + \sum_{n=1}^{N} \sum_{d=1}^{D} \sum_{m=1}^{M} E_{d,m}^n \tag{13}$$

subject to:

$$\sum_{l=1}^{L} \sum_{m=1}^{M} \epsilon_{u,l,m}^n + \sum_{d=1}^{D} \sum_{m=1}^{M} \zeta_{u,d,m}^n = 1 \quad \forall\, u, n \tag{14}$$

$$\sum_{d=1}^{D} \sum_{m=1}^{M} \zeta_{u,d,m}^n R_{u,d,m}^n + \sum_{l=1}^{L} \sum_{m=1}^{M} \epsilon_{u,l,m}^n R_{u,l,m} \geq R_u^{\text{th}} \quad \forall\, u, n \tag{15}$$

$$R_u^{th} \Big(\sum_{u=1}^{U} \sum_{m=1}^{M} \epsilon_{u,l,m}^n + \overline{U}_l^n \Big) \leq R_{GBS}^{\max} \quad \forall\, l, n \tag{16}$$

$$R_u^{th} \Big(\sum_{u=1}^{U} \sum_{m=1}^{M} \zeta_{u,d,m}^n \Big) \leq R_{DBS}^{\max} \quad \forall\, d, n \tag{17}$$

$$\kappa_d^n < 1 + \frac{\sum_{u=1}^{U} \sum_{m=1}^{M} \zeta_{u,d,m}^n}{Q} \quad \forall\, d, n \tag{18}$$

$$\kappa_d^n \geq \frac{\sum_{u=1}^{U} \sum_{m=1}^{M} \zeta_{u,d,m}^n}{Q} \quad \forall\, d, n \tag{19}$$

$$\mathbf{J}_d^{\min} \leq \mathbf{J}_d^n \leq \mathbf{J}_d^{\max}, \quad \forall\, d, n \tag{20}$$

$$\kappa_d^n, \zeta_{u,d,m}^n, \epsilon_{u,l,m}^n \in \{0, 1\} \tag{21}$$

Constraint (14) forces UE u to be associated with DBS d or GBS l. Constraint (15) indicates that the rate of UE u, which is associated to either DBS d or GBS l, is lower bounded by a threshold rate R_u^{th}. Constraints (16) and (17) define an upper bound for the maximum rate for GBS and DBS, respectively, given that $\overline{U}_l^n$ is the number of UEs served by GBS l at time block n. Since κ_d^n indicates whether DBS d is used in time block n or not, constraints (18) and (19) are used to extract this information from $\zeta_{u,d,m}^n$ where when $\zeta_{u,d,m}^n = 0$ then consequently $\kappa_d^n = 0$ and when $\zeta_{u,d,m}^n = 1$ for any UE u and resource block M then $\kappa_d^n = 1$ which means that DBS d is used during time block n. Note that Q is a very large number. Constraint (20) is used to limit the 2D coordinates of DBS d where $\mathbf{J}_d^{\min} = [x_d^{\min}, y_d^{\min}]^T$ and $\mathbf{J}_d^{\max} = [x_d^{\max}, y_d^{\max}]^T$. Finally, constraint (21) is defining our binary decision variables to be 0 or 1.

$\mathbf{P1}$ is not easy to solve due to the following: 1) the decision variables κ_d^n, $\zeta_{u,d,m}^n$, $\epsilon_{u,l,m}^n$ are binary and thus the objective function (29) and constraints (14)-(19) involve integer constraints. 2) Even if we fixed the decision variables, constraint (15) is still non-convex with respect to DBS coordinates variable $\mathbf{J}_d^n$. Therefore, problem (29) is mixed-integer nonlinear non-convex problem, which is difficult to be solved optimally.

B. Proposed Solution

In general, $\mathbf{P1}$ has no standard method for solving it efficiently. In the following, we propose an efficient iterative algorithm for solving $\mathbf{P1}$. Specifically, for a given coordinate $\mathbf{J}_d^n$, we optimize the decision variables, i.e. ζ, κ and ϵ, by solving a Linear Program (LP) after relaxing the decision variables. For any given ζ, κ and ϵ, the DBS coordinates $\mathbf{J}_d^n$ are optimized based on the successive convex approximation technique [12]. Finally, an iterative algorithm is given to solve $\mathbf{P1}$ efficiently.

1) Solving for Decision Variables: By fixing the DBS coordinates, the resulting problem will be an Integer Linear Programming (ILP) which can be solved optimally but not efficiently due to the large number of binary variables. In this case, relaxing the binary variables and then reconstructing them will allow us to solve this problem efficiently. Hence, for any given DBS coordinates $\mathbf{J}_d^n$, the variables of $\mathbf{P1}$ can be optimized by solving the following relaxed problem:

$$(\mathbf{P2}): \underset{\epsilon_{u,l,m}^n, \zeta_{u,d,m}^n, \kappa_d^n}{\text{minimize}} \quad \sum_{n=1}^{N} \sum_{l=1}^{L} E_l^n + \sum_{n=1}^{N} \sum_{d=1}^{D} E_d^n \tag{22}$$

subject to:

$$\text{Constraints}(14) - (19)$$

$$0 \leq \kappa_d^n, \zeta_{u,d,m}^n, \epsilon_{u,l,m}^n \leq 1 \quad \forall\, u, d, l, n \tag{23}$$

Note that in $\mathbf{P2}$, $R_{u,d,m}^n$ is not a variable anymore since we fixed the DBS coordinates. The relaxed $\mathbf{P2}$ is an LP which can be solved using any LP solver.

2) Solving for DBS Coordinates: For any given decision variable (to avoid infeasibility, $\mathbf{P2}$ is solved first then the optimal decision variables from $\mathbf{P2}$ are used in this problem), the DBS coordinates $\mathbf{J}_d^n$ can be optimized by solving the following problem:

$$(\mathbf{P3}): \underset{\mathbf{J_d^n}}{\text{minimize}} \quad \sum_{n=1}^{N} \sum_{l=1}^{L} E_l^n + \sum_{n=1}^{N} \sum_{d=1}^{D} E_d^n \tag{24}$$

subject to:

$$\text{Constraints}(15), (20)$$

In $\mathbf{P3}$, Constraints (14), (16)-(19) and (21) are not involved in $\mathbf{P3}$ since the decision variables are now fixed and their values are iteratively updated from $\mathbf{P2}$. The objective function and all constraints of $\mathbf{P3}$ are convex except for constraint (15). This constraint is neither concave nor convex with respect to the DBSs' coordinates which appears in $R_{u,d,m}^n$. It is worth notingthat the second term of the same constraint is not a function of the DBSs' coordinates, hence it is linear. Returning back to the first term of constraint (15), call it $\tilde{R}$, which can be expanded as follows:

$$\tilde{R} = \sum_{d\in\mathcal{D}}\sum_{m\in\mathcal{D}} \zeta^{n}_{u,d,m}\log_2\Big(1+\frac{\frac{p_{d,m}\ \rho_o}{h^2+||\mathbf{J}^n_d-\mathbf{g}_u||^2}}{\sum\limits_{\substack{j\in\mathcal{D}\\ j\neq d}}\frac{p_{j,m}\ \rho_o}{h^2+||\mathbf{J}^n_j-\mathbf{g}_u||^2}+\sigma^2}\Big)$$

$$\sum_{d\in\mathcal{D}}\sum_{m\in\mathcal{D}} \zeta^{n}_{u,d,m}\log_2\Big(\frac{\sum_{j\in\mathcal{D}}\frac{p_{j,m}\rho_o}{h^2+||\mathbf{J}^n_j-\mathbf{g}_u||^2}+\sigma^2}{\sum\limits_{\substack{j\in\mathcal{D}\\ j\neq d}}\frac{p_{j,m}\ \rho_o}{h^2+||\mathbf{J}^n_j-\mathbf{g}_u||^2}+\sigma^2}\Big)$$

$$= \sum_{d\in\mathcal{D}}\sum_{m\in\mathcal{D}} \zeta^{n}_{u,d,m}\Big(\underbrace{\log_2\big(\sum_{j\in\mathcal{D}}\frac{p_{j,m}\rho_o}{h^2+||\mathbf{J}^n_j-\mathbf{g}_u||^2}+\sigma^2\big)}_{\tilde{R}^1}$$

$$\underbrace{-\log_2\big(\sum_{\substack{j\in\mathcal{D}\\ j\neq d}}\frac{p_{j,m}\ \rho_o}{h^2+||\mathbf{J}^n_j-\mathbf{g}_u||^2}+\sigma^2\big)\Big)}_{\tilde{R}^2} \tag{25}$$

Our main goal is to convert Eq. (25) to a concave form in order for $\mathbf{P3}$ to be convex. Both terms of $\tilde{R}$, i.e., $\tilde{R}^1$ and $\tilde{R}^2$ are neither concave nor convex. $\tilde{R}^2$ is not concave with respect to $\mathbf{J}^n_j$, however, it is concave with respect to $||\mathbf{J}^n_j-\mathbf{g}_u||^2$. This motivates us to introduce the slack variable $\mathbf{\Psi}=\{\Psi^n_{u,j}=||\mathbf{J}^n_j-\mathbf{g}_u||^2, \forall j\in\mathcal{D}, j\neq d, u, n\}$ to make $\tilde{R}^2$ concave in $\mathbf{\Psi}$. After introducing this slack variable to $\tilde{R}^2$, we have to add a new constraint to $\mathbf{P3}$ which is expressed as [13]:

$$\Psi^n_{u,j}\leq||\mathbf{J}^n_j-\mathbf{g}_u||^2 \qquad \forall j\in\mathcal{D}, j\neq d, u, n \tag{26}$$

Back to the first term of $\tilde{R}$, i.e., $\tilde{R}^1$, this term is neither concave nor convex. Even with the slack variable, $\tilde{R}^1$ will not be concave (it will be convex). To tackle the non-concavity of $\tilde{R}^1$, the successive convex approximation technique can be applied where in each iteration, the original function is approximated by a more tractable function at a given local point. Define $\mathbf{J}^n_d(r)$ as the given DBS d location in the r-th iteration. Recall that $\tilde{R}^1$ is convex in $||\mathbf{J}^n_j-\mathbf{g}_u||^2$ and since any convex function can be globally lower-bounded by its first order taylor expansion at any point [14], hence, given $\mathbf{J}^n_d(r)$ in iteration r, we obtain the following lower bound for $\tilde{R}^1$:

$$\tilde{R}^1 \geq\log_2\Big(\sum_{j\in\mathcal{D}}\frac{p_{j,m}\rho_o}{h^2+||\mathbf{J}^n_j(r)-\mathbf{g}_u||^2}\Big)$$
$$-\sum_{j\in\mathcal{D}}Z^n_{u,d}(||\mathbf{J}^n_j-\mathbf{g}_u||^2-||\mathbf{J}^n_j(r)-\mathbf{g}_u||^2)=\tilde{\tilde{R}}^1 \tag{27}$$

where $Z^n_{u,d}$ is constant which is given by:

$$Z^n_{u,d}=\frac{\frac{p_{j,m}\rho_o}{h^2+(||\mathbf{J}^n_j(r)-\mathbf{g}_u||^2)^2}\log_2(e)}{\sum_{k\in\mathcal{D}}\frac{p_{k,m}\rho_o}{h^2+||\mathbf{J}^n_k(r)-\mathbf{g}_u||^2}+\sigma^2} \tag{28}$$

After using Successive convex approximation with $\tilde{R}^1$ and using a slack variable with $\tilde{R}^2$, now Eq.(25) is concave. Hence, with any given local point $\mathbf{J}^n_j(r)$, problem $\mathbf{P3}$ can be approximated to $\overline{\mathbf{P3}}$ as follows:

$$(\overline{\mathbf{P3}}):\underset{\mathbf{J^n_d},\mathbf{\Psi^n_{u,j}}}{\text{minimize}}\qquad \sum_{n=1}^{N}\sum_{l=1}^{L}E^n_l+\sum_{n=1}^{N}\sum_{d=1}^{D}E^n_d \tag{29}$$

subject to:

$$\sum_{d=1}^{D}\sum_{m=1}^{M}\zeta^n_{u,d,m}\Big(\tilde{\tilde{R}}^1-\log_2\big(\sum_{\substack{j\in\mathcal{D}\\ j\neq d}}\frac{p_{j,m}\ \rho_o}{h^2+||\mathbf{J}^n_j-\mathbf{g}_u||^2}+\sigma^2\big)\Big)$$
$$+\sum_{l=1}^{L}\sum_{m}^{M}\epsilon^n_{u,l,m}R_{u,l,m}\geq R^{\text{th}}_u \quad \forall\ u,n \tag{30}$$

$$\Psi^n_{u,j}\leq||\mathbf{J}^n_j-\mathbf{g}_u||^2 \qquad \forall j\in\mathcal{D}, j\neq d, u, n \tag{31}$$

$$\mathbf{J}^{\text{min}}_d\leq\mathbf{J}^n_d\leq\mathbf{J}^{\text{max}}_d, \quad \forall\ d,n \tag{32}$$

Finally, we propose an iterative algorithm to solve $\mathbf{P1}$. The variables in $\mathbf{P1}$ are partitioned into two blocks, i.e., association and coordinates variables. Then they are alternately optimized (solving $\mathbf{P2}$ then $\overline{\mathbf{P3}}$ iteratively) while keeping the other variables fixed. Furthermore, the obtained solution in each iteration is used as the input to the next iteration. The details of this algorithm is summarized in Algorithm 1.

Algorithm 1: Iterative approximate solution for $\mathbf{P1}$

Input: $\mathbf{J}^n_d(0)$
Output: $\mathbf{J}^n_d(r+1), \kappa^n_d(r+1), \zeta^n_{u,d,m}(r+1), \epsilon^n_{u,l,m}(r+1)$

```
while r ≠ maximum iteration do
    Solve Problem P2 for given J_d^n(r).
    Reconstruct the binary variables, check their feasibility and
      then denote them as
      κ_d^n(r+1), ζ_{u,d,m}^n(r+1) and ε_{u,l,m}^n(r+1)
    Solve Problem P3‾ for given
      κ_d^n(r+1), ζ_{u,d,m}^n(r+1), ε_{u,l,m}^n(r+1).
    Denote the optimal solution of P3‾ as J_d^n(r+1)
    Update r=r+1
    if The fractional increase of the objective value ≤ ε^th then
        Break
    end
end
```

IV. Simulation Results

In this section, selected numerical results are provided to investigate the benefits of utilizing DBSs in mitigating BS failure in 5G networks. The simulation model consists of 5 GBSs where one of them fails, hence, we are considering one failure at a time. We initialized 4 standby DBSs to be used in case of the conventional self-healing approach can't accommodate the users originally served by the failed BS.

Table I System parameters

Parameter	Value	Parameter	Value	Parameter	Value
f (GHz)	2.1	R^{max}_{GBS} (bps/Hz)	100	$\mathbf{J}^{\text{min}}_d$ (m)	**-200**
$p_{d,m}$ (mW)	100	R^{max}_{DBS} (bps/Hz)	10	$\mathbf{J}^{\text{max}}_d$ (m)	**200**
$P_{l,m}$ (mW)	100	R^{th}_u (bps/Hz)	2	h_l (W)	30
σ^2 (dBm)	-80	β_d (W)	1	h_d (min)	100
T (min)	60	α_d	2.6	ρ_o	0.01
T_f (min)	0.5	α_l	4.7	Q	1000

Table II Association and rates for 10 UEs

UEs	Time block 1 (n=1)		Time block 2 (n=2)	
	Association	R (bps/Hz)	Association	R (bps/Hz)
UE1	GBS1	2.82	GBS1	2.28
UE2	GBS2	2.43	GBS2	2.66
UE3	DBS1	3.28	DBS4	3.59
UE4	GBS3	2.41	GBS3	2.33
UE5	DBS1	3.00	DBS4	3.37
UE6	GBS2	2.28	GBS2	2.25
UE7	GBS4	2.17	DBS4	3.12
UE8	GBS3	3.07	GBS3	2.71
UE9	DBS1	2.80	GBS1	2.30
UE10	GBS2	2.00	GBS2	2.00

The simulation area is 400x400 m^2 where the failed BS is centered at the origin and the UEs of the failed BS are distributed randomly over this area. The UEs of the failed BS are static, however, the number of users within each neighboring GBSs is changing randomly per time block. The parameters used to calculate P_{hov} and P_{har} are taken from [11]. In Table I, we present the remaining parameters used in the simulations.

Table 2 shows the users association (DBS or GBS) and rates for 10 UEs during 2 time blocks. The remaining time blocks are skipped for space limitations. For time block 1, only DBS 1 is used from a set of 4 DBSs and all other UEs are served by GBSs. Since DBS 1 is serving UE 3, UE5 and UE 9, their corresponding rates are relatively high. UE 1 is associated to the same GBS during time block 1 and 2, however, its rate decreased during time block 2. This is due to the change of the capacity of GBS 1 since GBS 1 has to its own UEs first and participate in the healing process by the available capacity. During time block 2, DBS 4 is serving UE 3, UE 5 and UE 9. According to these UEs' locations, DBS 4 optimizes its location to deliver the almost same rate to each of them.

Figure 3 shows the accumulated consumed energy for both DBSs and GBSs for different number of UEs. It is worth noting that the GBS energy is the excess energy consumed to serve the users originally served by the failed BS. This means that the energy consumed by any GBS to serve its own users is not accounted in our model. On the other hand, the energy consumed by the DBS is the hovering, hardware and communication power which is significantly high compared with the excess energy consumed by the GBS. As the number of UEs increases from 4 to 10, the number of used DBS is increasing since the GBSs are serving their own UEs and serving the targeted UEs using only the available capacity. At certain point, all DBSs are used to satisfy the target UEs minimum rate requirement. If the number of UEs kept increasing, the problem will not be visible since DBSs and GBSs will not be able to deliver the minimum requirement for number of UEs.

Fig. 4 shows different scenarios of the proposed scheme where there are 8 UEs was connected to the failed BS and there are 4 neighboring GBSs and 4 DBSs ready to participate in the healing process and subject to our main objective which is the energy minimization. In Fig. 4(a) the GBSs are serving all the UEs without any help from the DBSs. This occurs at the detection of the failure since the DBSs still didn't arrive to the designated locations or if the GBSs are non loaded with there own users and they can satisfy all UEs rate requirements. In Fig. 4(b), UE 3 and UE 7 are not achieving there minimum rate R_u^{th} by their association to GBS 4 and GBS 1, respectively. In this case these two UEs are associated to DBS 1. Although attaching them to DBS 1 will not reduce the energy, this will satisfy UE 3 and UE 7 threshold rates subject to constraint (15).

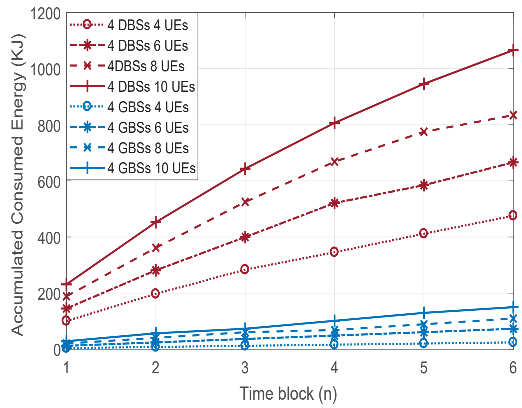

Figure 3: Accumulated energy for DBSs and GBSs.

Figure 4(c) shows how the proposed hybrid algorithm solved the main challenge of the conventional self-healing approach. In this scenario, GBS 4 is fully loaded with its own UEs in this case UE 7 will be associated to DBS 1 which already serving UE 3 and UE 5. If DBS 1 was not having enough capacity, then an additional DBS will be used. Finally, Fig. 4(d) shows a scenario where all GBSs are fully loaded and they are not able to associate any additional UEs. This scenario is subject to infeasibility based on the available capacity of the DBSs and the number of UEs need to be served. It worth noting to say that the 4th DBS was not involved in the healing process in all scenarios.

From the simulation results, we can infer that the hybrid COC is converted to the conventional COC approach if the GBSs are having enough capacity to serve the UEs of the failed BS. If the number of UEs increases, the disadvantage of the conventional approach will start to appear where either the GBS will not serve the target UE or will degrade the rate of its own UE. Using hybrid approach, we can avoid this scenario by using a DBS to serve those users. This prove that the proposed approach overcome the disadvantage of the conventional COC approach where the UEs of the neighboring GBSs are not affected by the failure and at the same time the UEs of the failed BS are getting continuous service.

There are number of challenges to practically implement the proposed hybrid approach. One of these challenges is the movement of a DBS from one location to another which is always considered to happen in no time. This challenge can be

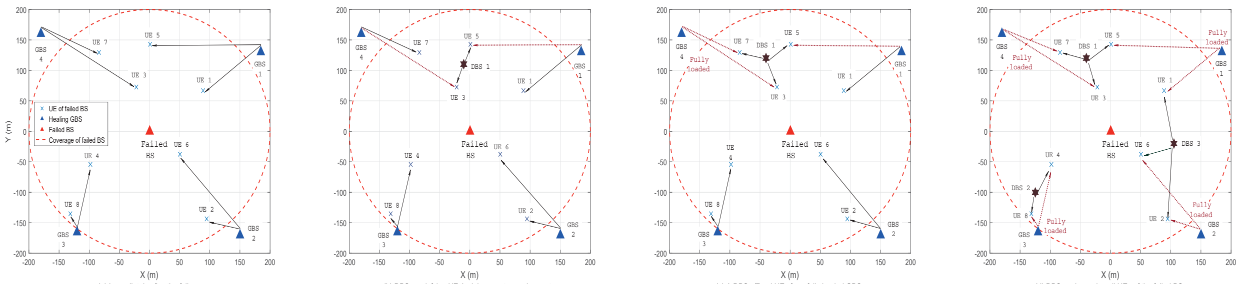

(a) Immediately after the failure (b) DBSs sarisfying UEs' minimum rate requirement (c) A DBS offload UEs from fully loaded GBS (d) DBSs only serving all UEs of the failed BS

Figure 4 : Cell outage compensation different scenarios (GBSs COC, hybrid COC and DBSs COC) with 4 DBSs, 4 GBSs and 8 UEs.

tackled by adding a velocity constraint to limit the movement of the DBS to its maximum speed which we are considering in our future extension of this work.

V. Conclusion

In this paper, we proposed a novel cell outage compensation (COC) approach for 5G networks assisted by Drone Base-Stations (DBSs). The objective is to minimize the total energy consumption of the DBSs and Ground Base-stations (GBSs) while maintaining the minimum quality of service requirements of the users that are originally served by the failed BS. DBSs are optimally managed in order to serve the users that can not be served by GBSs while considering DBSs consumed energy. The simulation results show how this hybrid COC approach outperforms the conventional COC approach. The proposed hybrid approach shows significant impacts on ensuring connectivity of the users originally served by the failed BS while minimizing the number of used DBSs.

References

[1] Y. Zeng, R. Zhang, and T. J. Lim, "Wireless communications with unmanned aerial vehicles: Opportunities and challenges," IEEE Communications Magazine, vol. 54, no. 5, pp. 3642, May 2016.

[2] O. G. Aliu, A. Imran, M. A. Imran, B. Evans, "A Survey of Self Organisation in Future Cellular Networks," IEEE Comm. Surveys & Tutorials, vol.15, no.1, pp.336-361, 2013.

[3] M. Selim, A. E. Kamal, K. Elsayed, H. M. Abdel-Atty and M. Alnuem, "Fronthaul cell outage compensation for 5G networks," in IEEE Communications Magazine, vol. 54, no. 8, pp. 169-175, August 2016.

[4] S. Rohde, M. Putzke, and C. Wietfeld, Ad-hoc self-healing of OFDMA networks using UAV-based relays, Ad Hoc Networks, vol. 11, no. 7, pp. 18931906, Sep. 2013

[5] A. Merwaday and I. Guvenc, UAV assisted heterogeneous networks for public safety communications, in Proc. IEEE Wireless Commun. and Netw. Conf. Workshops (WCNCW), Mar. 2015, pp. 329334.

[6] M. Mozaffari, W. Saad, M. Bennis and M. Debbah, "Drone Small Cells in the Clouds: Design, Deployment and Performance Analysis," 2015 IEEE Global Communications Conference (GLOBECOM), San Diego, CA, 2015, pp. 1-6.

[7] J. Lyu, Y. Zeng, R. Zhang, "UAV-Aided Cellular Offloading: A Potential Solution to Hot-Spot Issue in 5G", available online "httpss://arxiv.org/abs/1705.09024".

[8] A. Al-Hourani, S. Kandeepan and A. Jamalipour, "Modeling air-to-ground path loss for low altitude platforms in urban environments," 2014 IEEE Global Communications Conference, Austin, TX, 2014, pp. 2898-2904.

[9] Y. Zheng, Y. Wang and F. Meng, "Modeling and Simulation of Pathloss and Fading for Air-Ground Link of HAPs within a Network Simulator," 2013 International Conference on Cyber-Enabled Distributed Computing and Knowledge Discovery, Beijing, 2013, pp. 421-426.

[10] G. Auer, O. Blume, V. Giannini, I. Godor, M. Imran, "Energy efficiency analysis of the reference systems, areas of improvements and target breakdown," Energy Aware Radio and Network Technologies, Dec. 2010.

[11] A. Alsharoa, H. Ghazzai, A. Kadri and A. E. Kamal, "Energy Management in Cellular HetNets Assisted by Solar Powered Drone Small Cells," 2017 IEEE Wireless Communications and Networking Conference (WCNC), San Francisco, CA, 2017.

[12] T. Wang and L. Vandendorpe, "Successive convex approximation based methods for dynamic spectrum management", IEEE International Conference on Communications (ICC), Ottawa, ON, 2012.

[13] Q. Wu, Y. Zeng, R. Zhang, "Joint Trajectory and Communication Design for Multi-UAV Enabled Wireless Networks", available online "https://arxiv.org/abs/1705.02723".

[14] S.Boyd and L. Vandenberghe, Convex Optimization. Cambridge University Press, 2004.